SAND20XX-XXXXR
LDRD PROJECT NUMBER: 19-1069
LDRD PROJECT TITLE: Tunable Thermal Transport across Interfaces via Phonon Engineering
PROJECT TEAM MEMBERS: Chris Saltonstall (6755), Elbara Ziade (9144), Khalid Hattar (1882), Thomas Beechem (1878)

ABSTRACT: The influence of He ion radiation on GaAs thermal conductivity was investigated using TDTR and the PGM. We found that damage in the shallow defect only regions of the radiation profile scattering phonons with a frequency to the fourth dependence due to randomly distributed Frankel pairs. Damage near the end of range however, scatters phonons with a second order frequency dependence due to the cascading defects caused by the rapid radiation energy loss at the end of range resulting in defect clusters. Using the PGM and experimental thermal conductivity trends it was then possible to estimate the defect recombination rate and size of defect clusters. The methodology developed here results in a powerful tool for interrogating radiation damage in semiconductors.

INTRODUCTION: Gallium arsenide (GaAs) remains a vital electronic material for communications applications including radar, cellular and satellite applications. GaAs has advantages over Si in these areas due to its high saturation velocity and higher electron mobility, which enable GaAs devices to operate at several hundred GHz while its larger bandgap acts to reduce electrical noise. High speeds, currents, and powers offered by GaAs also necessitate the ability to dissipate the substantial thermal energy produced in their use.

GaAs has a comparatively small thermal conductivity, however, having an intrinsic value (~40 W/mK) that is ~3.5 times smaller than silicon (~150 W/mK). Furthermore, GaAs is often utilized in high altitude applications—such as communication satellites--where the material is continually bombarded by cosmic radiation. Radiation, in turn, induces defects in the GaAs that will reduce its thermal conductivity and thus the ultimate capability of devices based on their use. In response, we examine the magnitude of radiation induced reductions in the thermal conductivity of GaAs while simultaneously highlighting the utility of irradiation in probing phonon-defect interactions.

Radiation degrades GaAs owing to the variety of defects and impurities created during ion implantation. As radiative ions enter GaAs, they are slowed by frequent electron scattering and infrequent nuclear collisions leading to randomly spaced Frankel pairs, which are composed of a single defect and an interstitial atom. Ultimately, some fraction of these Frankel pairs result in a distribution of anti-site defects. Near the end of range, the ion rapidly decelerates and becomes implanted from a series of cascading nuclear collisions. These cascading collisions create

Sandia National Laboratories is a multimission laboratory managed and operated by National Technology and Engineering Solutions of Sandia, LLC, a wholly owned subsidiary of Honeywell International, Inc., for the U.S. Department of Energy's National Nuclear Security Administration under contract DE-NA-0003525.

clusters of defects and interstitials similar to an amorphous ``grain". Additionally, implanted noble gases are immiscible in GaAs and therefore can cluster into nanoscale ``bubbles" at the end of range. Each type of defect and impurity acts to reduce the thermal conductivity by scattering phonons but to different extents. Understanding the sensitivity of thermal conductivity and phonon scattering to each of these defect and impurity types is our aim.

Despite the maturity of thermal science, assessing the impact of individual defect structures on thermal conductivity remains relatively unassessed. From a computational perspective, modeling individual defects requires large simulation cells to create realistic defect densities and quasi-random distributions. Large cells, in turn, are computationally expensive and therefore infrequently employed. Experimental measurements of thermal conductivity, meanwhile, sample all defects "at once" oftentimes precluding the isolation of individual effects. Ion irradiation circumvents these problems as energy and dose allow for specific defects to be purposely dialed in.

For these reasons, we use He radiation to examine the comparative impact of point and cluster defects on the thermal conductivity of GaAs. Using TDTR with variable modulation frequency, the thermal properties of different radiation induced defect regions are separately investigated. Scattering near the surface is dominated by a fourth order frequency dependence indicating randomly distributed point defects (anti-site, interstitials and vacancies). In contrast, phonon scattering near the end of range region exhibits a second order frequency dependence indicative of "grains" created by damage clusters. Together, these results suggest that He impurities at the energy and fluences studied have a relatively small effect on phonon scattering compared to the defects caused by their implantation. Ion implantation thus serves not only as a tool to examine sensitivity of material systems to environmental conditions but as a scalpel useful in isolating particular phonon-defect scattering events. Together, the thermal results are consistent with electronic studies of radiation damage, which report cascading defects near the end of range and isolated defects near the surface.

DETAILED DESCRIPTION OF EXPERIMENT/METHOD:

SAMPLES

Undoped zinc blende (100) GaAs substrates purchased from AXT were irradiated with helium ions at fluences ranging from 2e11 to 2e16 ions/cm^2 at 300 keV. Crystal defects were induced via ion beam irradiation in GaAs (100) ±0.5^o orientation single crystals using a 3 MV Pelletron from National Electrostatics Corporation ion beam irradiation.

Stopping and Range of Ions in Matter calculations were done in Quick Calculation mode using a lattice binding energy of zero, threshold displacement energy of 18 eV, and a density of 5.32 g/cm^3.

When the calculations were repeated in Full Cascade mode, the vacancy concentrations were approximately twice that of Quick Calculation mode, as expected. The total defect concentration cannot be determined by SRIM, as it neglects defect recombination. Thus, the irradiation fluences were selected based on the peak vacancy concentration, vacancies/cm^3, as calculated by SRIM, while minimizing the implanted helium concentration to avoid helium bubble formation. Samples irradiated with 300 keV He received $2.1x10^{11}$ - $2.1x10^{16}$ ions/cm^2 ($5x10^{17}$ - $5x10^{22}$ vacancies/cm^3), and samples irradiated with 800 keV He received $2.2x10^{11}$ - $2.2x10^{16}$ ions/cm2 ($5x10^{17}$ - $5x10^{22}$ vacancies/cm3). The vacancy peak was located at approximately 1.2 µm from the surface with 300 keV He as shown in Fig. 1. The total damage range extended to approximately 1.7 µm with 300 keV He.

The peak He concentration reached 1.2 atomic percent at the highest doses at both irradiation energies. All of the implants were done into polished single crystal GaAs wafers purchased from AXT and diced into 1 cm^2 pieces, then mounted on a Si background using carbon tape for irradiation. The sample stage was tilted to 3^o during irradiation to avoid ion channeling effects, which would shift the peak depth in the damage profile away from the SRIM calculated value. An effort was made to minimize alterations in the damage rate between samples by keeping a constant ion flux, but, due to the wide range of fluences and limited beamtime, the flux was gradually increased with fluence. Ion fluxes were approximately the same for both ion beam energies, and varied with fluences as follows: $5x10^{10}$ ions/cm2/s (fluence = $2x10^{11}$ ions/cm^2), $5x10^{11}$ ions/cm^2/s (fluences = $2x10^{12}$ -$2x10^{13}$ ions/cm^2), $3x10^{12}$ ions/cm^2/s (fluence = $2x10^{14}$ ions/cm^2), and $2x10^{13}$ ions/cm^2/s (fluences = $2x10^{15}$ - $2x10^{16}$ ions/cm^2). The sample holder was cooled to keep the samples close to room temperature, which ranged from 13 to 25 ^{o}C during the highest flux irradiation.

Alcohol and plasma cleaning procedures to minimize cracked hydrocarbon contamination were implemented to ensure the best quality Raman and TDTR measurements.

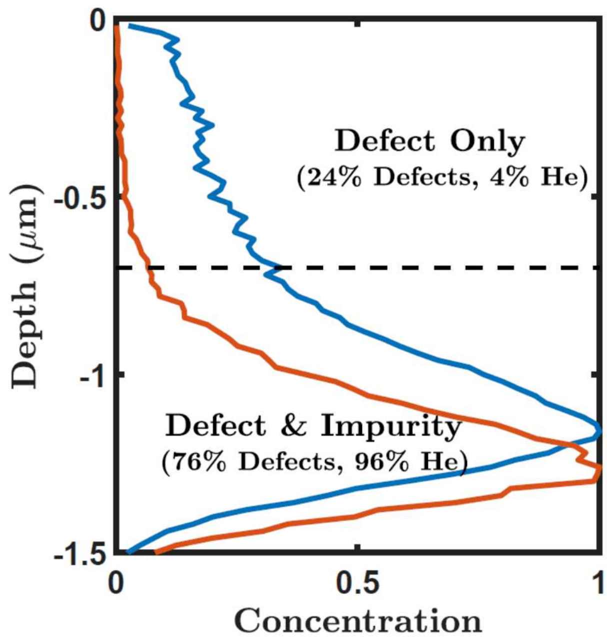

Figure 1: SRIM simulations of defect (blue) and He (red) impurity profiles from 300 keV He radiation in GaAs. Concentration is normalized to the peak intensities which scales linearly with radiation fluence. Peak concentration of defects and He impurities at 2e11 cm^2 fluence is 5.7e17 cm^3 and $1.3e^7$ cm^{-3}, respectively. Radiation profile was delineated (dashed line) into two regions for the thermal model. “Defect Only” region contains 24% and 4% of the total defects and He inclusions while the “Defect and Impurity” region contain 76% and 96% of the total defects and He inclusions.

RAMAN SPECTROSCOPY

Crystal structure after radiation was characterized using Raman spectroscopy. The optical penetration depth of 532 nm light is only 93 nm in crystalline GaAs and decreases with disorder. Therefore, a Raman signal could only be collected from the top "defect only" region. Due to the polar nature of GaAs, the longitudinal optical (LO) Raman signal is not purely from the vibrational modes but is influenced by free electron plasmon leading to a longitudinal optical plasmon coupled (LOPC) mode. Therefore, the LO peak at approximately 292 cm^{-1} was fit using the LOPC model.

THERMAL MEASUREMENTS

Thermal conductivity was measured using time domain thermo-reflectance (TDTR). The TDTR system used is describe in detail else ware. Measurements were collected with a 6 and 40 micron $1/e^2$ radius spot at 20 and 40 mW powers for the probe and pump, respectively. Temperature measurements were collected in Janis cryostat at $1e^{-8}$ Torr to prevent condensation at low temperatures.

Sandia National Laboratories is a multimission laboratory managed and operated by National Technology and Engineering Solutions of Sandia, LLC, a wholly owned subsidiary of Honeywell International, Inc., for the U.S. Department of Energy’s National Nuclear Security Administration under contract DE-NA-0003525.

The TDTR model assumes a finite number of discrete homogeneous films. Therefore, we approximated the irradiated GaAs sample as two homogeneous films shown in Fig. 1 on an unirradiated substrate. The top 0.67 µm thick “defect only” layer thermal conductivity was probed with a modulation frequency of 11.3 MHz. This value was held constant and the bottom 0.83 µm thick “defect and impurity” layer was probed at 3.37 MHz. The bulk substrate layer was determined from the control sample and its thermal conductivity was held constant for all irradiated samples.

PHONON GAS MODEL

The experimental data was modeled using the phonon gas model (PGM) with a similar methodology as Beechem *et al*. Here we use the real dispersion of GaAs in the Γ-X direction and make the isotropic assumption. The maximum wavevector was scaled to maintain the correct number of modes in the Brillouin zone. However, the group velocities were calculated at each *k*-point before scaling to prevent erroneous velocity values. Umklapp scattering rate coefficients were determined by fits to experimental GaAs data. Scattering rate coefficients from radiation induced damage were determined by fits to data from this work as will be discuss later.

RESULTS:

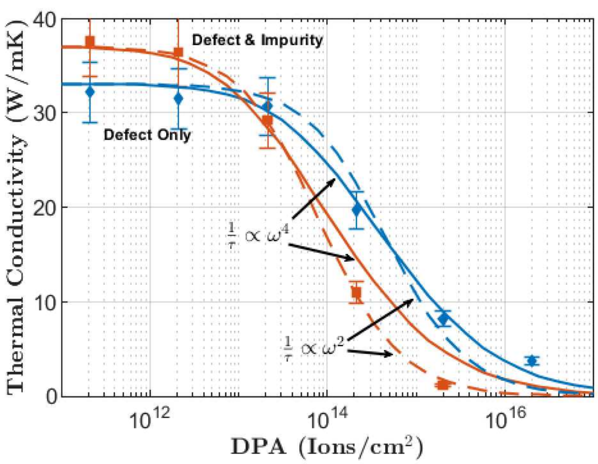

Figure 2: Thermal conductivity is plotted as a function of He radiation fluence (ions/cm^2) for the “defect only” region (diamonds) and “defect and impurity” region (squares) as described in Fig. 1. The PGM was fit to the experimental data using a radiation scattering rate equation, Eq. 1 assuming 4th order point defect scattering (solid lines) and 2nd order line defect scattering (dashed lines) from radiation defects. Sensitivity was lost to the “defect and impurity” region at highest radiation dose and so this data point was excluded.

Sandia National Laboratories is a multimission laboratory managed and operated by National Technology and Engineering Solutions of Sandia, LLC, a wholly owned subsidiary of Honeywell International, Inc., for the U.S. Department of Energy’s National Nuclear Security Administration under contract DE-NA-0003525.

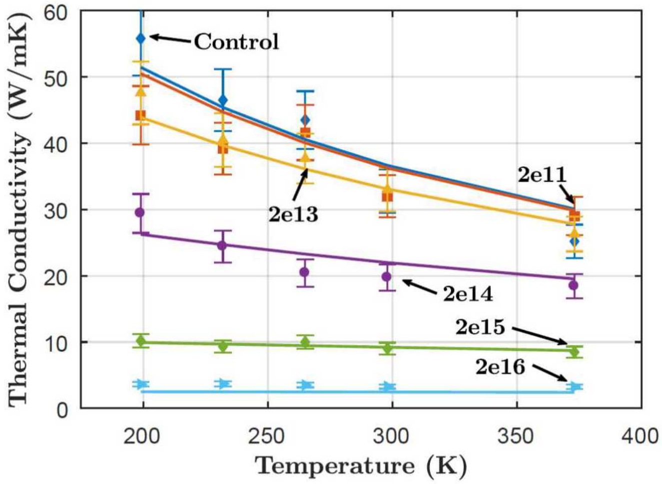

Figure 3: *Temperature dependent thermal conductivity of the "defect only" region at various fluences from experiment (markers) and predicted (solid lines) using the PGM with scattering rate coefficient from Table~\ref{tbl:scatter}*

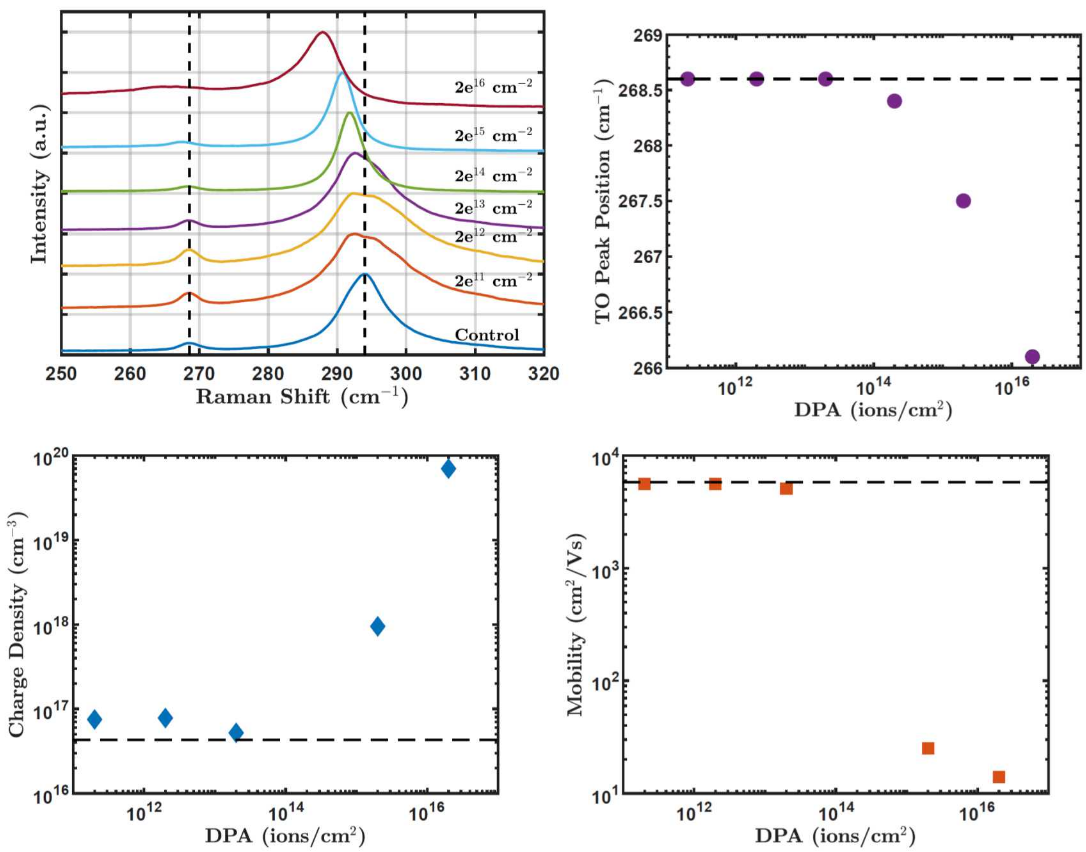

Figure 4: *(a) Raman spectra of He irradiated GaAs at various fluences. The Raman penetration depth in GaAs using a 532 nm laser is at maximum 300 µm and so the spectra are representative of the "defect only" region described in Fig. 1. Vertical*

dashed lines are guides to the eye for peak position changes. The (b) TO peak position, (c) charge density and (d) electron mobility which were extracted from the LO peak remain relatively constant up to fluences of 2e13 ion/cm². However, above 2e13 ion/cm² each property rapidly changes. Horizontal dashed lines represent unirradiated (control) values.

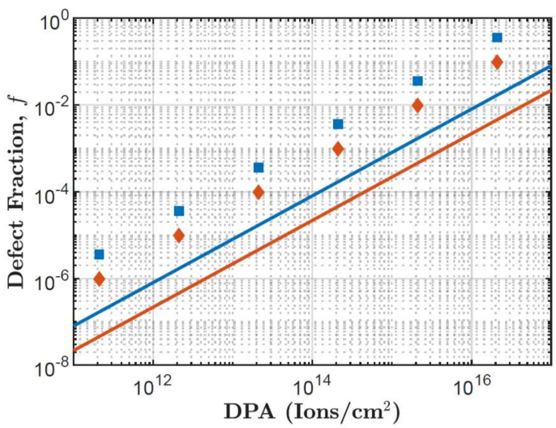

Figure 5: Defect fraction predicted from (markers) SRIM and (solid lines) Eqs. 4 and 6 for the (blue) defect only region and (red) defect and impurity region.

DISCUSSION:

The thermal conductivity follows a sigmoidal trend with radiation dose as shown in Fig. 2. At low irradiation fluences, the thermal conductivity is unaffected until a critical dose is reached. Above this point, the thermal conductivity precipitously decreases until asymptotically approaching a minimum thermal conductivity which is speculated to be the amorphous limit, ~1 W/mK. Even at the highest fluence the "defect only" region does not become fully amorphous as indicated by the relatively high thermal conductivity and Raman spectra. The thermal conductivity of approximately 1 W/mK in the "defect and impurity" region suggests that it may have become fully amorphous. However, the penetration depth of the Raman spectra was not deep enough to confirm this.

Table 1: Scattering rate parameters for fit of the "defect only" region (DOR) and the "defect and impurity" region (DIR).

	$A_{n=4}$ (s^3cm^{-2}/ions)	$A_{n=2}$ (s cm^{-2}/ions)	B (s/K)	C (K)
DOR	6e-58	1.8e-29	2.57e-19	86.82
DIR	2e-59	9e-29	2.2e-19	86.82

The critical fluence where the thermal conductivity begins to decrease depends on irradiated layer. For the "defect only" region, the thermal conductivity drops off above 2e13 cm^{-2}. The "defect and impurity" region on the other hand begins to decrease at nearly an order of magnitude lower dose, 2e12 cm^{-2}. This could be attributed to the increased defect density and additional He impurities. However, there are only three times as many defects in the ``defect and impurity" region and the maximum He concentration is only $2.8e^{-11}$ percent of the GaAs atomic density. It is well known that some types of disorder create point defect type scattering while other can create glassy type scattering. Therefore, the difference in trend magnitude could be due to different types of scattering mechanisms due different types of disorder.

The scattering mechanisms in the two regions were investigated using the phonon gas model (PGM) described above. The influence of irradiation damage induced scattering was accounted for using,

$$1/\tau = AD\omega^n \tag{1}$$

where D is the irradiation dose in units ions/cm^{-2}, ω is the radial phonon frequency and A is a fitting parameter. The exponent, n, was selected as 2 or 4 to model grain boundaries and point defects, respectively. Initially, it was assumed that irradiation would create point defects. This assumption holds for the "defect only" region as the fit using $n = 4$ captures the thermal conductivity trend with irradiation dose well while $n = 2$ does not as shown in Fig. 2. However, the point defect assumption could not capture the trend in the "defect and impurity" region instead the grain boundary assumption needed to be used. This implies that the type of defect created by He ion radiation changes as the ion approaches the end of range. This also suggest that He impurities have little effects on scattering mechanisms since isolated He defects would scatter phonons with a fourth order frequency dependence.

The implication that different defect types are present in the two regions is supported by previous studies of radiation damage in semiconductors. Before the end of range, radiation damage creates Frankel pairs from sparse random ion-atom scattering. Since these Frankle pairs are isolated and nearly uniformly randomly spaced, they behave like point defects and scatter phonon with an ω^4 dependence. Near the end of range, however, the ions quickly lose energy from a rapid series of cascading scattering events. This results in a dense network of extended defect loops and clusters\cite{williams1998aa} which scatter phonons with an ω^2 dependence.\cite{klemens1958aa}

The assumption of point defect type scattering in the "defect only" region is further supported by temperature dependent thermal conductivity trends shown in Fig. 3. At low radiation doses below 2e14 cm^{-2}, the thermal conductivity decreases with temperature due to Umklapp scattering with magnitudes mostly constant at all temperature and doses. At doses equal to 2e14 cm^{-2} and above, the magnitudes begin to decrease, and the temperature trends begin to flatten. These changes are similar to those seen in binary alloys indicating a fourth order frequency dependent point defect type scattering.

RAMAN CHARACTERIZATION

Raman spectra of He irradiated GaAs at various doses are plotted in Fig. 4 a). Within the region of the LO-phonon mode at 292 cm^{-1}, the spectral response changes drastically as a function of dose. Qualitatively, the energy of the mode first increases with irradiation until a dose rate of 2e14 cm^{-2} where it returns to its "rest" position. Additional dosing then induces a net energy reduction of the mode. These changes are indicative of the disorder's effect on both the electronic and lattice environments and thus give insight into mechanisms driving thermal conductivity reduction.

In polar semiconductors, the LO-phonon mode couples with the charge carriers via plasmon-phonon coupling. The position of the so-called longitudinal optical plasmon coupled (LOPC) mode is dependent upon not only the phonon energy but also its lifetime along with the free carrier concentration and mobility. Here, we leverage this dependence to assess the changes in doping and mobility that occur with irradiation. Practically, each spectrum was fit using the sum of two spectral features. The first took the shape of either an over- or under-damped LOPC depending upon the position of the maximum relative to the LO-phonon. Values higher (lower) than the LO-phonon indicate an under- (over-) damped plasmon where electron scattering occurs at a rate less (greater) than the plasma frequency. A second Voigt function having a constant peak position of 292 cm^{-1} was also used to account for the surface depletion region that emerges from interaction of the GaAs with its native oxide.

The multi-parametric least squares fitting procedure is not determinant for each of the parameters. It does, however, provide a bound for the mobility and doping concentration. Practically, these bounds were arrived at by taking the fitted function and then individually the ranges over which the coefficient of variance changed by less than 0.1% near its maximum of >0.99.

Quantitatively, the fitting provides insight into changes in the electronic transport environment with the irradiation. Quantitatively, charge carriers are seen to increase after the critical dose of $1x10^{13}$ cm^{-2} in conjunction with a drastic mobility decrease. Each indicates a substantial degree of induced disorder within the near surface region prior to the end of range. Increased doping, for instance, occurs in GaAs with the introduction of vacancies, Frankel pairs that are induced with irradiation. Reductions in mobility, meanwhile, highlight the increased scattering with disorder. Taken together, the results emphasize the presence of disorder at depths substantially less than the end of range supporting the analysis of thermal transport containing a "shallow" disorder only region and an additional "end of range" region in which disorder and impurities are prevalent.

The shape of the Raman spectra also provides qualitative insight into the magnitude of disorder. The Raman spectra of fully amorphous semiconductors closely resembles that materials vibrational density of states while the periodic phase yields sharp symmetric spectral features.

The irradiated GaAs spectra below 2e14 cm^{-2} fluences show complex features due to the electronic effects making them difficult to use as metrics for disorder. The spectra at fluences of 2e14 cm^{-2} fluences and above, however, results from the vibrational states. The relatively sharp and symmetric peaks combined with the shift in peak position and electron mobility at 2e14 and 2e15 cm^{-2} doses indicate that the shallow "defect only" region is mostly ordered but with significant defects. At the highest radiation fluence, 2e16 cm^{-2}, both peaks significantly broaden and become asymmetric indicating the onset of strong disorder. However, the spectrum still does not resemble the vibrational density of states which suggests that the "defect only" region never becomes fully amorphous.

ESTIMATING DEFECT DENSITY

Thus far we have utilized thermal properties to characterize the dominate defect structures in the two radiation regions of GaAs. Utilizing these fits along with scattering theory it is also possible to estimate defect densities.

In the defect only region, we found that the primary defects were point defects. These point defects come in the form of Ga and As interstitials, vacancies and anti-site defects (swapped Ga and As). The scattering rate predicted for the combination of these defect types can be modeled by,

$$\frac{1}{\tau} = \frac{V_0}{\pi \bar{v}^3} \sum_i f_i \left(\frac{\delta v_i}{v}\right)^2 \omega^4, \tag{2}$$

where,

$$\left(\frac{\delta v_i}{v}\right)^2 = \frac{1}{4}\left[\left(1 - \frac{M_i}{\overline{M}}\right)^2 + 2\left\{6.4\gamma\left(1 - \frac{R_i}{\overline{R}}\right)\right\}^2\right] \tag{3}$$

V_0 is the primitive cell volume, v is the average sound speed, ω is the phonon radial frequency, $\bar{M}$ and $\bar{R}$ are the average atomic mass and radius, respectively, γ is the Gruniesen parameter, f_i is the number of defects per primitive cell and the summation is over the i^{th} defect type. Assuming anti-site defects are negligible, one interstitial results in one vacancy, and interstitials and vacancies have equivalent scattering strengths, the summation can be removed (see Appendix for detailed discussion). The point defect fraction, f, can then be determined as a function of dose by setting the coefficient of Eq. 1 equal to the ω^4 coefficient in Eq. 2, yielding

$$f = \frac{\pi \bar{v}^3 AD}{V_0}\left(\frac{\delta v}{v}\right)^{-2}. \tag{4}$$

Sandia National Laboratories is a multimission laboratory managed and operated by National Technology and Engineering Solutions of Sandia, LLC, a wholly owned subsidiary of Honeywell International, Inc., for the U.S. Department of Energy's National Nuclear Security Administration under contract DE-NA-0003525.

A similar methodology was used by Cahill to estimate defect concentrations in irradiated InN. However, they used a simplified thermal conductivity formalism derived for temperatures well above the Debye limit which is not the case for GaAs at room temperature (θ_D = 360 K). Therefore, this methodology resulted in unphysical defect estimates and is not presented here.

Figure 5 plots the average defect concentration of the defect only region versus radiation dose as predicted by SRIM simulations and Eq. 4. Both methods predict a linear defect concentration with radiation dose due to the linearly increasing number of radiation ions. However, Eq. 4 predicts approximately 95% few defects than SRIM. This is likely due to the change in defect concentration from spontaneous recombination. Interstitial defects are meta-stable at formation and will therefore migrate to nearby vacancies at finite temperature to annihilate the defect or create anti-site defects. The 95% recombination rate predicted here is consistent with literature lending credence to the use of TDTR as a probe for radiation defects.

In addition to point defects, this methodology can be used estimate the structure and concentration of amorphous grains in the defect and impurity region. Turk and Klemens derived a relationship for the phonon scattering rate due to impurity platelets, i.e., clusters of defects/impurities,

$$\frac{1}{\tau} = \frac{8h}{\overline{v}} \frac{\pi R_p^2 h}{V_p} \left(\frac{\delta v}{v}\right)^2 \omega^2 I(z), \tag{5}$$

Where R_p is the platelet radius, h is the platelet height and I(z) is a function of Bessel functions. Using a similar methodology as for Eq. 4 and assuming h = $2R_p$, the individual defect fraction can be solved for,

$$f = \frac{AD\overline{v}}{16R_p} \left(\frac{\delta v}{v}\right)^{-2}. \tag{6}$$

Equation 6 is a function of one unknown parameter, the cluster radius, R_p. However, if we assume that the recombination rate is an intrinsic material property, it must be approximately the same in the defect and impurity region as it is for the defect only region, $f_{DOR} \approx f_{DIR}$. This assumption allows us to estimate the size of the defect clusters caused by a single He ion strike, R_p = 1.8 nm.

ANTICIPATED OUTCOMES AND IMPACTS:

- Presentations and Publications
  - Two papers in preparation for publication in PRB
- Tools and Capabilities
  - Added high frequency capabilities to frequency domain thermo-reflectance (FDTR) enabling sensitivity to ultra thin material layers.
  - Added two color capabilities to FDTR enabling material measurement flexibility
  - Repair time domain thermo-reflectance TDTR.

- Staff development
    - First experience as PI in proposal development and project leadership
        - Two early career staff
            - Elbara Ziade (140 hr)
            - Chris Saltonstall (111 hr)
        - Two graduate students
            - Chris Perez (169 hr)
            - Ethan Scott (137 hr)
    - Academic collaboration with University of Virginia (UVa)
- *Key technical accomplishment*
    - Identified that ion irradiation can be used to localize phonons enabling crystalline materials to have thermal conductivity near the amorphous limit. Opens pathways for thermoelectric and **phonon glass – electron crystals** material design.
- *Plans for follow-on and partnerships*
    - Vehicle technology office wide band-gap power electronics initiative (Funded $100k FY20)
    - Plan to submit to LDRD (NM)
    - Engaging with Sandia customers for future work
        - 5800 – microelectronics reliability in radiation environments
        - 6700 – optimizing thermal transport in satellites
        - 1800 – optimizing thermal transport in wide band gap devices

CONCLUSION:

The influence of He ion radiation on GaAs thermal conductivity was investigated using TDTR and the PGM. We found that damage in the shallow defect only regions of the radiation profile scattering phonons with a frequency to the fourth dependence due to randomly distributed Frankel pairs. Damage near the end of range however, scatters phonons with a second order frequency dependence due to the cascading defects caused by the rapid radiation energy loss at the end of range resulting in defect clusters. Using the PGM and experimental thermal conductivity trends it was then possible to estimate the defect recombination rate and size of defect clusters. The methodology developed here results in a powerful tool for interrogating radiation damage in semiconductors.

Sandia National Laboratories is a multimission laboratory managed and operated by National Technology and Engineering Solutions of Sandia, LLC, a wholly owned subsidiary of Honeywell International, Inc., for the U.S. Department of Energy's National Nuclear Security Administration under contract DE-NA-0003525.

Sandia National Laboratories

U.S. DEPARTMENT OF ENERGY